Heliospheric plasma sheets

N. U. Crooker,[1] C.-L. Huang,[1] S. M. Lamassa,[1] D. E. Larson,[2] S. W. Kahler,[3] and H. E. Spence[1]

Received 30 July 2003; revised 17 October 2003; accepted 17 December 2003; published 26 March 2004.

[1] As a high-beta feature on scales of hours or less, the heliospheric plasma sheet (HPS) encasing the heliospheric current sheet shows a high degree of variability. A study of 52 sector boundaries identified in electron pitch angle spectrograms in Wind data from 1995 reveals that only half concur with both high-beta plasma and current sheets, as required for an HPS. The remaining half lack either a plasma sheet or current sheet or both. A complementary study of 37 high-beta events reveals that only 5 contain sector boundaries while nearly all (34) contain local magnetic field reversals, however brief. We conclude that high-beta plasma sheets surround current sheets but that most of these current sheets are associated with fields turned back on themselves. The findings are consistent with the hypothesis that high-beta plasma sheets, both at and away from sector boundaries, are the heliospheric counterparts of the small coronal transients observed at the tips of helmet streamers, in which case the proposed mechanism for their release, interchange reconnection, could be responsible for the field inversions. *INDEX TERMS:* 2164 Interplanetary Physics: Solar wind plasma; 2134 Interplanetary Physics: Interplanetary magnetic fields; 2169 Interplanetary Physics: Sources of the solar wind; 2109 Interplanetary Physics: Discontinuities; *KEYWORDS:* sector boundary, heliospheric current sheet, magnetic holes

Citation: Crooker, N. U., C.-L. Huang, S. M. Lamassa, D. E. Larson, S. W. Kahler, and H. E. Spence (2004), Heliospheric plasma sheets, *J. Geophys. Res.*, *109*, A03107, doi:10.1029/2003JA010170.

1. Introduction

[2] A plasma sheet is generally viewed as a sheath encasing a current sheet, where the sheath is distinguished from its surroundings by elevated density. In the case of the heliosphere, with its global heliospheric current sheet (HCS) serving as a magnetic equatorial plane between sectors of opposite polarity, *Burlaga et al.* [1990a] designated the heliospheric plasma sheet (HPS) as the equatorial solar wind sandwiched between high-speed streams from the magnetic polar regions of the Sun. The boundaries of this HPS are marked by stream interfaces on the leading and trailing edges of those streams [cf. *Burton et al.*, 1999]. By analogy to the plasma sheet in Earth's magnetotail, this HPS is associated with closed field line regions of the Sun and comprises a considerable volume of the heliosphere. Appropriate as the name ''heliospheric plasma sheet'' is for this feature, common usage now dictates that it be called the ''slow wind'' instead, meaning what was originally slow wind when it left the Sun, as opposed to fast wind from coronal holes [cf. *Schwenn*, 1990; *Geiss et al.*, 1995].

[3] On scale sizes two orders of magnitude smaller than those considered by *Burlaga et al.* [1990a], *Winterhalter et al.* [1994] designated the HPS as a minutes-long high-beta feature encasing the HCS, where beta is the ratio of gas to field pressure. Their analysis focused on a set of 19 well-defined, isolated HCS crossings selected from more than a year of ISEE 3 data. Each HPS was roughly in pressure balance with its surroundings, with a decrease in field pressure balanced primarily by an increase in density and, hence, gas pressure.

[4] Other studies using elevated density as the primary HPS signature derived double scale sizes for the structure, with an hours-long core immersed in a broad halo [*Bavassano et al.*, 1997; *Wang et al.*, 1998; *Lacombe et al.*, 2000]. Through superposed epoch analysis, *Borrini et al.* [1981] and *Gosling et al.* [1981] were the first to demonstrate that the HCS is imbedded in a pronounced density peak, which they interpreted as the extension of coronal streamers into the heliosphere. *Bavassano et al.* [1997] recognized the core-halo structure of the density peak in their studies of time variations of Helios data and proposed that it was the heliospheric counterpart of a core-halo coronal streamer structure deduced from radio occultation measurements. Their sketch of the structure shows a dense stalk $1°–2°$ wide extending from the cusp of a helmet streamer imbedded in a less dense halo $15°–20°$ wide extending radially from the base of the helmet. *Wang et al.* [1998] sketched essentially the same coronal structure based upon coronagraph observations of white light variations and reached the same conclusion regarding the double structure of the HPS.

[5] Whereas most of the studies cited above treat the HPS as a steady state structure, *Wang et al.* [2000, p. 25,133] formed their idea of the HPS based upon observations of

[1]Center for Space Physics, Boston University, Boston, Massachusetts, USA.
[2]Space Sciences Laboratory, University of California, Berkeley, Berkeley, California, USA.
[3]Air Force Research Laboratory, Hanscom Air Force Base, Massachusetts, USA.

0148-0227/04/2003JA010170$09.00

small-scale plasma transients: ''Time-lapse sequences...indicate that streamers are far more dynamic than was previously thought, with material continually being ejected at their cusps and accelerating outward along their stalks.'' *Wang et al.* [1998, 2000] go so far as to propose that the entire HPS consists of discontinuous plasma parcels, possibly released when an open field line reconnects with a closed field line, a process called ''interchange reconnection'' by *Crooker et al.* [2002]. Further, *Wang et al.* [1998, 2000] suggest that the straight rays observed in the vicinity of helmet streamers are the legs of these recently opened field lines, continuing to release plasma from what was originally the helmet streamer.

[6] The dynamic view of streamers advanced by *Wang et al.* [1998, 2000] had been proposed earlier for their heliospheric extensions by *Crooker et al.* [1993]. In a subsequent case study of an HCS crossing accompanied by multiple high-beta plasma sheets, *Crooker et al.* [1996a] showed that the data were inconsistent with multiple encounters with a single wavy HPS and suggested that the structures were transients. This paper builds on that study by taking a synoptic approach to the problem, analyzing the nature of the HPS on successive crossings of sector boundaries over a 7 month period. In addition, this paper surveys high-beta events and tests for HPS characteristics. Preliminary results from these studies were reported by *Crooker* [2003]. Here the completed studies are presented and discussed in terms of solar sources.

[7] Of primary importance to these studies is the use of suprathermal electrons to identify a sector boundary, here defined as the boundary between magnetic fields of true opposite polarity at their solar origins [*Crooker et al.*, 1996b; *Kahler et al.*, 1996]. With use of higher-energy electrons, *Kahler and Lin* [1994, 1995] first demonstrated how electrons continually streaming away from the Sun along magnetic field lines give incontrovertible remote information about the direction of those field lines as they leave the Sun. If the electrons stream parallel to the field, the field line is connected to the Sun with away polarity, even if it is locally inverted and points toward the Sun. Likewise, if electrons stream antiparallel to the field, the field line is connected to the Sun with toward polarity. Applying these criteria, *Kahler and Lin* [1994, 1995] found two patterns: reversals in local field polarity unaccompanied by true sector boundaries as identified in the electron data and true sector boundaries unaccompanied by reversals in local field polarity. The former pattern is easily understood in terms of a current sheet formed by a local field inversion, where the field turns back on itself. This paper shows that such field inversions are common properties of high-beta events away from sector boundaries. The latter pattern, however, i.e., true sector boundaries without local field reversals, has defied interpretation until recently. Now, *Crooker* [2003] and *Crooker et al.* [2004] (hereinafter referred to as Paper 2) offer explanations in terms of a variety of three-dimensional configurations of field inversions intrinsic to sector boundaries. Unique to these configurations is a local diversion of the HCS from the true sector boundary. While not the subject of this paper, it is helpful to keep this possibility in mind when confronted in section 2 with cases of noncoincidence of the three elements required for a steady state plasma sheet, namely, a sector boundary, a current sheet, and a high-beta or high-density event.

2. Analysis

[8] The Wind data used for this study are from late 1994 through 1995, during the declining phase of the solar cycle, when the spacecraft was immersed in a relatively stable two-stream, four-sector recurrence pattern [e.g., *Crooker et al.*, 1996c]. Solar wind ion and magnetic field data, merged at the 92 s cadence of the ion data (courtesy of the MIT Space Plasma Group), were obtained from the Solar Wind Experiment (SWE) [*Ogilvie et al.*, 1995] and the Magnetic Field Investigation (MFI) [*Lepping et al.*, 1995], respectively, and electron spectrograms were obtained from the Three-Dimensional Plasma and Energetic Particle Experiment (3DP) [*Lin et al.*, 1995].

2.1. Plasma Sheets at Sector Boundaries

[9] The starting point for our HPS survey was to identify all sector boundaries in the period from 14 December 1994 to 31 July 1995, after which the spectrograms become increasingly difficult to read owing to interference from electrons accelerated at Earth's bow shock, as noted by *Szabo et al.* [1999]. Spectrograms of 320 eV electrons were inspected for changes in the direction of the magnetic field-aligned beam or strahl from parallel to antiparallel to the field or vice versa. The resulting list of true sector boundaries is shown in Table 1. The numbering system in the first two columns identifies 34 consecutive, major boundaries between global-scale sectors, seven of which have lettered multiple boundaries. Regarding the latter, the list is conservative rather than exhaustive. Boundaries marking excursions into the opposite sector lasting less than 1 hour were not included, nor were any that occurred in regions where the strahl was too weak to detect changes in direction relative to the field. A comparison with sector boundaries identified by *Lacombe et al.* [2000] in total electron heat flux variations suggests that some multiple or intrasector boundary crossings may have been missed, especially in July, although inspection of the spectrograms indicates that some of these show no change in strahl direction relative to the field and that some are associated with counterstreaming [cf. *Kahler et al.*, 1996].

[10] The third and fourth columns of Table 1 give the date and time of each sector boundary crossing. Some of the times are finite intervals. These intervals either lack strahls or, in cases 13 and 27, cover data gaps, but the true polarity is opposite on either side, implying at least one reversal within. The data gap in case 27 is more than 1 day long, adding uncertainty to plasma sheet identification, but it is included for completeness.

[11] The fifth column of Table 1 lists whether or not a current sheet coincides with each sector boundary. As mentioned in the introduction, noncoincidence of sector boundaries identified in electron data and magnetic field changes signaling current sheets was first noted by *Kahler and Lin* [1994, 1995]. By ''current sheet,'' we mean a current structure associated with a reversal in the longitude angle ϕ_B of the local magnetic field from one sector to the other, in the same sense as in the electron data, where the field sectors are centered on the average Parker spiral

Table 1. Sector Boundaries

Major	Minor	Date	Time, UT	CS?	β PS?	β Scale, hours	*n* Scale, hours	β HPS?
1	a	14 Dec. 1994	1720	yes	no		9	no
	b		2045	no	yes	3	"	no
	c		2320	no	no		"	no
2	a	17 Dec. 1994	1920	no	yes	0.25, 4.5	16	no
	b	18 Dec. 1994	715	no	no		"	no
	c		1720–1930	no	no		"	no
3		23 Dec. 94	0640–700	yes	∼yes	4	4	∼yes
4		2 Jan. 1995	0425	yes	no		2, 12	no
5		10 Jan. 1995	2000	yes	yes	0.33, 1.5	0.33, 3	yes
6		16 Jan. 1995	1220	no	no		12	no
7		20 Jan. 1995	∼2200	∼yes	no		4	no
8		28 Jan. 1995	2215	no	no		12	no
9		6 Feb. 1995	∼0525	yes	∼yes	0.5	0.5, 17	∼yes
10		8 Feb. 1995	0405–0615	no	no			no
11		16 Feb. 1995	1640 to ∼2200	yes	yes	0.03, 5	5	yes
12		25 Feb. 1995	1430	∼yes	no			no
13		4 March 1995	1900 (3 March) to 2100 (4 March)	yes	yes	0.25, 5	2, 5	yes
14		9 March 1995	0230	yes	yes	0.17	0.33, 2	yes
15	a	16 March 1995	2010 to 0520 (17 March)	yes	yes	0.5, 2.5	2.5	yes
	b	17 March 1995	0815–0920	yes	yes	1	1	yes
	c		1840–2125	yes	yes	2.5	2.5	yes
16		25 March 1995	2100 (25 March) to 0900 (26 March)	yes	yes	8, 17	15	yes
17	a	30 March 1995	1110	yes	no		6	no
	b	31 March 1995	0420	no	yes	3	15	no
	c		0700–0715	no	yes	3	"	no
	d		1835	yes	yes	3	3	yes
	e		2125	yes	yes	3	"	yes
18	a	5 April 1995	1230	no	yes	6	15	no
	b		1755	no	yes	6	"	no
	c		2045	no	no		"	no
19		15 April 1995	0440	yes	yes	2	2, 12	yes
20	a	18 April 1995	1040–1620	yes	yes	6	6	yes
	b	21 April 1995	0820–1030	no	no			no
	c	22 April 1995	0850–0910	yes	no		8	no
21		25 April 1995	1855–2200	yes	yes	1, 7		yes
22		2 May 1995	0340–0355	yes	no		1, 9	no
23		12 May 1995	1820–2310	yes	yes	0.17, 5	6	yes
24		16 May 1995	0945	∼yes	no		12	no
25		23 May 1995	0300–1400	yes	yes	11	11	yes
26		29 May 1995	0720	no	no		14	no
27		8 June 1995	0800 (10 June) to 1300	yes	yes	3		yes
28		14 June 1995	0740	yes	yes	1, 13		yes
29	a	17 June 1995	1440–1750	yes	yes	0.42		yes
	b		1920–2000	yes	yes	1, 6	2	yes
	c		2140	yes	yes	0.67		yes
	d	18 June 1995	0200–0230	yes	no			no
	e	19 June 1995	0740–0815	yes	yes	1	1, 4	yes
30		25 June 1995	1225–1240	yes	∼yes	0.17, 1	1	∼yes
31		2 July 1995	0520–0820	no	no			no
32		9 July 1995	1450–2030	yes	yes	5	9	yes
33		11 July 1995	∼2300	no	no			no
34		23 July 1995	1900 (24 July) to 0335	∼yes	∼yes	12		∼yes

longitudes of 135° and 315°. To qualify as concurrent, the field must pass through either boundary of these sectors, at 45° or 225°, within 15 min of the true sector boundary identified in the electron data or, in the case of a listed interval for the true sector boundary, within that interval. The three cases marked "∼yes" fit this pattern, but ϕ_B briefly returns to its original sector within the hour, even though the electron data indicate no additional polarity change. Thus these cases are immediately followed by intervals of fields turned back on themselves.

[12] The sixth column of Table 1 lists whether or not the sector boundary is immersed in a high-beta structure or plasma sheet (β PS), where here "plasma sheet" is used in its most general sense as a feature with an elevated beta and/or density. Those marked "∼yes" are marginal, either because the rise in beta is minor compared to rises in surrounding structures or because the structure borders rather than encases the sector boundary. The seventh column lists a scale size for the high-beta structure, two in cases with pronounced nested structure. Since these pressure balance structures occur over a wide range of scale sizes [e.g., *Burlaga et al.*, 1990b], the listed sizes are only those most obvious when scanning the data by eye. The eighth column gives similar scale sizes for any high-density (*n*) structures at the sector boundary. As discussed below, most of these are different from the beta scale sizes owing to the dominant role of magnetic field strength in governing the beta profile. The density structures can be considered as high-density plasma sheets, but only scale sizes less than 1 day are listed in order to document the kinds of plasma

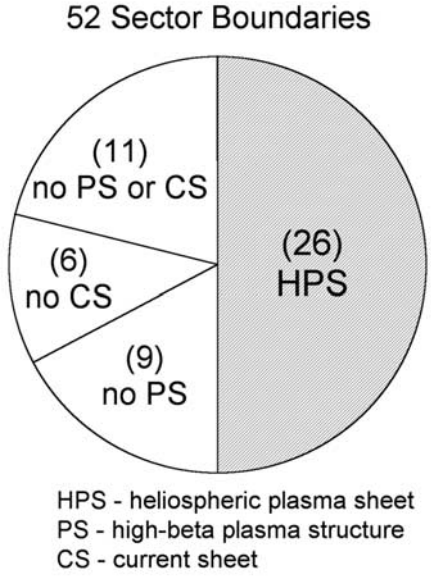

Figure 1. Distribution of plasma sheet properties at sector boundaries.

sheets found by *Bavassano et al.* [1997]. The larger scales sizes associated with the plasma sheets defined by *Burlaga et al.* [1990a] are not of interest here because they constitute the slow wind and so encompass all sector boundaries.

[13] The last column of Table 1 lists whether or not the sector boundary fits the definition of a heliospheric plasma sheet of the type identified by *Winterhalter et al.* [1994] but with no preselection for well-defined, isolated HCS crossings. We require coincidence of sector boundary, current sheet, and high-beta structure, as envisioned for a steady state HPS.

[14] The results listed in Table 1 are summarized in a pie chart in Figure 1. Of the total of 52 sector boundaries identified in electron data, counting individually all multiple boundaries, only half can be classified as high-beta HPSs. The remaining half lack either a current sheet (six have no CS) or a high-beta structure (nine have no PS) or both (11 have no PS or CS). Examples of these configurations are illustrated in Figure 2.

[15] Figure 2a illustrates an HPS of the type selected by *Winterhalter et al.* [1994]. It is the most pristine of the 52 cases. The electron spectrogram in the top panel shows strong strahl flux (red) switching abruptly from 0° to 180° in pitch angle, marking passage from an away sector to a toward sector at the vertical dashed line. In the second panel a sharp reversal in ϕ_B from the away to the toward Parker spiral direction coincides with the electron signature. The third panel shows a coincident, singular, 10 min spike in ion beta, and the fourth panel shows a similar spike in density n anticorrelated with a spike-like decrease in field strength B, or magnetic hole, accounting for the beta spike. The density spike rides on a broader, 2 hour density structure.

[16] In contrast to the pristine HPS signature in Figure 2a, Figure 2b illustrates a more typical HPS and thus the high degree of variability within the HPS category. The spectrogram shows a brief (~1 hour) interval of nearly isotropic pitch angle distributions sandwiched between the switch in strahl pitch angle marking passage from a toward to an away sector. The exact sector boundary location is assumed to coincide with the reversal in ϕ_B near the right edge of the isotropic interval, as marked by the vertical dashed line. Subsequently, ϕ_B returns to the toward sector (across both the 45° and 225° boundaries) several times before settling into an away orientation consistent with the electron signature, implying brief intervals of inverted fields. The third panel shows that the sector boundary coincides with a minor 20 min beta peak imbedded in a 1.5 hour peak centered on the large-angle ϕ_B excursion following the sector boundary. A broader 3 hour peak in density in the fourth panel spans the sector boundary and roughly anticorrelates with field strength; but the narrower width of the beta peak is controlled by the width of the dip in field strength.

[17] Figure 2c shows a pair of sector boundaries, neither of which coincide with a current sheet. Both boundaries are well-defined in the spectrogram, marking a 12 hour excursion into the toward sector, but the second panel shows that ϕ_B remains in the away sector across each one. Away from the sector boundaries, ϕ_B makes a much briefer ~2.5 hour excursion into the toward sector, but these local polarity reversals are not sector boundaries as defined by the electrons. It is as if there are ~5 hour mismatches between the true sector boundaries and their respective current sheets, where the intervals of mismatch contain fields turned back on themselves [cf. *Crooker*, 2003; Paper 2]. The third panel shows two pronounced high-beta structures, the first of which encompasses the first sector boundary. The second high-beta structure, however, encompasses not the second sector boundary but rather the ϕ_B excursion into the toward sector. The second sector boundary borders a minor peak in beta that was considered too marginal to classify as a high-beta plasma sheet. The fourth panel shows a broad density structure that essentially encompasses both sector boundaries but only marginally, at its borders. The center of the density peak, like that of the largest beta peak, coincides with the ϕ_B excursion into the toward sector. The field magnitude, again, as in Figure 2b, roughly anticorrelates with density but reflects far more the considerably different shape of the beta curve.

[18] Having thus covered examples of the Figure 1 categories of a sector boundary coincident with a high-beta plasma sheet and current sheet (HPS), with only a plasma sheet (no CS), and with neither plasma sheet nor current sheet (no PS or CS), we turn to Figure 2d for an example of the remaining category, a sector boundary coincident with only a current sheet (no PS). The sector boundary identified in the spectrogram aligns with a well-defined current sheet marked by a sharp reversal in ϕ_B in the second panel but falls between two peaks in beta in the third panel. The second beta peak is pronounced, covers minor excursions of ϕ_B to the opposite sector, and centers on a broad peak in density. In this case, as in Figure 2c, there is a pronounced plasma sheet encasing some kind of current structure that is displaced from the sector boundary.

[19] If high density instead of high beta is treated as the criterion required for an HPS, similar results are obtained. Minor differences between high-beta and high-density plasma sheets are that the latter have larger scale sizes, as

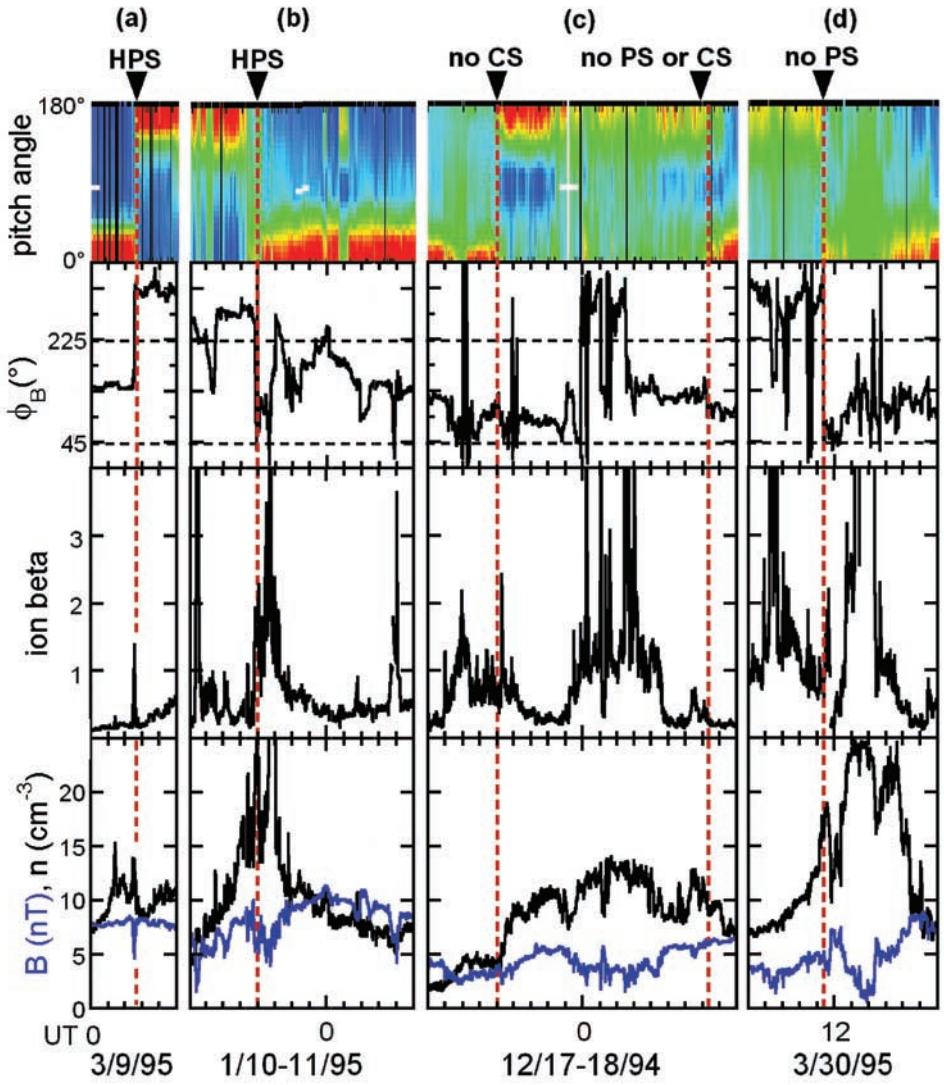

Figure 2. Time variations of 92 s values of the magnetic longitude angle ϕ_B (GSE coordinates, second panel), ion beta (third panel), and density n and field strength B (fourth panel) across sector boundaries identified in the 320 eV electron spectrograms (top panel) and marked by dashed red lines. Abscissa ticks mark hours. The four time intervals illustrate cases of (a) a simple heliospheric plasma sheet (HPS), defined by concurrence of a sector boundary, a high-beta plasma structure (PS), and a current sheet (CS), (b) an HPS with a complicated CS, (c) a sector boundary with a PS but no CS and a sector boundary with neither, and (d) a sector boundary with a CS but no PS.

is apparent in Figure 2, and, partly as a result of larger size, more often encompass sector boundaries. From Table 1, counting multiple sector boundaries embedded in the same high-density plasma sheet (the eight marked by quotation marks) only once, we find the following statistics: Of 44 (52−8) sector boundaries, 26 (59%) can be classified as HPSs (compared to 50% for high-beta plasma sheets), 6 lack just current sheets, 8 lack just plasma sheets, and 4 lack both current and plasma sheets. Irrespective of the current sheet requirement for an HPS, 73% (32/44) of sector boundaries are imbedded in (small scale) high-density plasma sheets compared to 62% (32/52) in high-beta plasma sheets. These two kinds of plasma sheets do not always occur together, as Table 1 attests. There are six sector boundaries embedded in high-beta plasma sheets with no high-density plasma sheets. (These can occur when the relative increase in density balancing the decrease in field strength is minimal owing to already elevated density and low field strength.) Conversely, there are 14 sector boundaries embedded in high-density plasma sheets with no high-beta plasma sheets.

[20] The scale-size distributions of high-density and high-beta plasma sheets, again irrespective of the current sheet requirement for an HPS, are compared in Figure 3. The values are taken from Table 1, including both scales for cases with two. As expected from the examples in Figure 2, the high-beta plasma sheets have shorter durations than the high-density plasma sheets, with median values of 2 and 3 hours, respectively. While Table 1 lists a few cases where the beta and density scales match, as would be expected for

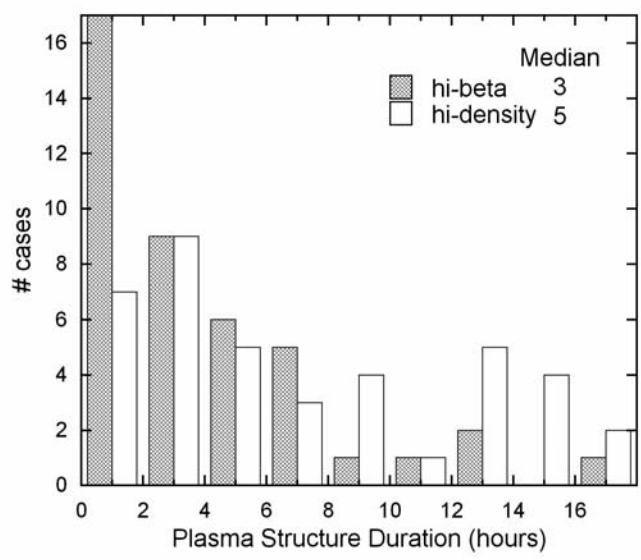

Figure 3. Distribution of high-beta and high-density plasma sheet durations.

a plasma sheet that is a simple pressure balance structure, in most cases the pressure balance structure that controls the profile of the high-beta structure is nested in a larger high-density structure so that the relative increase in density balancing the decrease in field strength does not stand out as a prominent density feature.

2.2. High-Beta Structures

[21] In performing the survey of sector boundaries discussed in section 2.1, it became clear that high-beta structures were not at all unique to sector boundaries and often encompassed current sheets. For example, in Figure 2b, one beta spike precedes the sector boundary by 3.5 hours and one follows by 8 hours, the latter accompanied by a sharp excursion of ϕ_B to the opposite sector. In addition, as discussed in section 2.1, the most pronounced beta peaks in Figures 2c and 2d occur away from the sector boundaries and coincide with ϕ_B excursions. To quantify the occurrence frequency of this pattern, we surveyed high-beta structures (plasma sheets) for sector boundaries and current sheets.

[22] Table 2 gives the results of the survey. The Wind data were searched for hours in which the average of ion beta exceeded 10, and these comprise the 37 listed cases. To obtain this many cases, the data were searched through the end of 1995 since only 11 cases were found through July, the interval used for the survey in section 2.1. The negative impact of bow shock contamination on sector boundary identification after July was less critical for this aspect of the study. Sector boundary identification, however, became somewhat problematical for another reason. There is a strong tendency for suprathermal electron pitch angle dis-

Table 2. High-Beta Structures

Date	Hour	SB?	CS?	Minimum B	Maximum n	High T or n	Entropy	HPS?
23 Dec. 1994	19	no	yes	1.2	49	n	low	no
16 March 1995	21	no	yes	0.4	14	n	low	no
16 March 1995	24	no	yes	0.2	14	both	low	no
30 March 1995	14–15	no	yes	0.3	25	both	low	no
31 March 1995	4	no	yes	0.4	18	n	low	no
17 May 1995	11	no	yes	0.2	20	n	low	no
23 May 1995	10	no	yes	0.3	47	both	low	no
29 May 1995	20–22	no	yes	0.7	14	T	high	no
17 June 1995	8	no	yes	0.4	13	T	low	no
4 July 1995	14	yes	yes	0.6	18	n	low	yes
6 July 1995	14	yes	yes	0.2	13	n	low	yes
16 Aug. 1995	1	no	no	0.2	4	T	high	no
19 Aug. 1995	14	no	yes	0.5	26	n	low	no
1 Sept. 1995	15	no	yes	0.3	23	n	low	no
2 Sept. 1995	21–22	no	yes	0.4	21	n	low	no
3 Sept. 1995	3	no	yes	0.3	15	T	low	no
4 Sept. 1995	10–11	no	no	0.4	22	both	low	no
13 Sept. 1995	7	no	no	0.7	5	both	high	no
19 Sept. 1995	14	no	yes	0.2	17	T	low	no
19 Sept. 1995	18	no	yes	0.4	28	T	low	no
20 Sept. 1995	10	no	yes	0.6	28	n	low	no
20 Sept. 1995	13	no	yes	0.4	31	both	low	no
20 Sept. 1995	15	no	yes	0.2	34	n	low	no
20 Sept. 1995	18–19	no	yes	0.1	25	n	low	no
25 Sept. 1995	18	no	yes	0.4	17	n	low	no
28 Sept. 1995	2	no	yes	0.4	13	both	medium	no
28 Sept. 1995	13	yes	yes	0.8	14	both	low	yes
15 Nov. 1995	2	no	yes	0.6	23	n	low	no
17 Nov. 1995	15–16	no	yes	0.2	20	n	low	no
18 Nov. 1995	1–3	no	yes	0.5	19	n	low	no
22 Nov. 1995	3	yes	yes	0.3	26	both	low	yes
3 Dec. 1995	3	no	yes	0.6	14	T	low	no
6 Dec. 1995	7	no	yes	0.4	6	T	medium	no
6 Dec. 1995	16	no	yes	0.2	15	both	low	no
15 Dec. 1995	15	yes	yes	1.2	52	n	low	yes
23 Dec. 1995	11	no	yes	0.3	10	both	medium	no
27 Dec. 1995	16	no	yes	0.2	6	both	medium	no

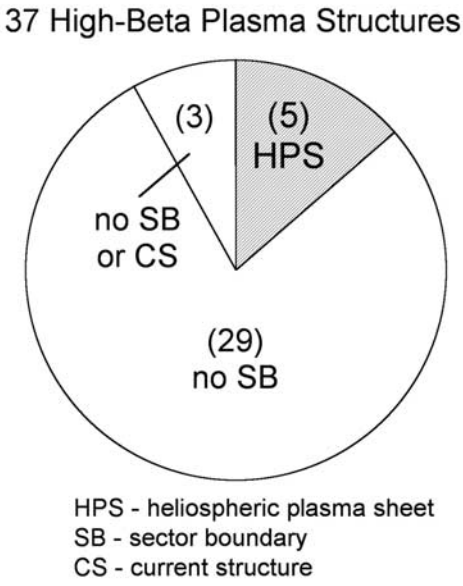

Figure 4. Distribution of plasma sheet properties in high-beta structures.

tributions to be isotropic in regions of high beta, as in Figure 2d [cf. *Zurbuchen et al.*, 2001]. Because of important implications of this tendency for topological interpretations of heat flux dropouts, another study was undertaken to document it [*Crooker et al.*, 2003]. The impact here is increased uncertainty in the third column of Table 2, which lists whether or not a high-beta structure encompasses a sector boundary. A sector boundary was assumed to be present if the true polarity was opposite on either side of the structure. In some cases the polarity determination had to be made well outside the event since relatively high beta and isotropy sometimes extend beyond the borders of the highest-beta regions. The most likely sector boundaries missed are any that occurred in pairs within the structures, leaving the same polarity on either side. (We note that in the period of overlap with Table 1 the two July sector boundaries listed in Table 2 do not appear in Table 1. Each of these is one of a pair of intrasector reversals with weak electron signatures that were routinely excluded from Table 1, as discussed in section 2.1.)

[23] The fourth column of Table 2 lists which high-beta structures encompass a current sheet. Although we used the same current sheet criterion as described in section 2.1, a sector change in ϕ_B, here "current structure" is a more appropriate term since usually the weak magnetic fields inside high-beta regions are highly disordered, often even more so than in the high-beta structure in Figure 2d [cf. *Zurbuchen et al.*, 2001; *Mullan et al.*, 2003]. The last column in Table 2 lists which high-beta structures can be classified as HPSs, i.e., which contain both a sector boundary and a current sheet.

[24] Similar to Figure 1, Figure 4 summarizes Table 2 results in the form of a pie chart. Only 5 of the 37 high-beta structures encompass sector boundaries. These comprise the five HPSs since they also encompass current sheets. While the remaining 32 high-beta structures lack sector boundaries, only 3 lack current sheets, as well. Irrespective of HPS classification, only 3 of the total of 37 lack current sheets. Thus one can conclude that nearly all high-beta structures are plasma sheets encompassing current sheets but that few of these coincide with sector boundaries.

[25] As a matter of supplemental interest, the fifth through eighth columns of Table 2 characterize the plasma in and surrounding the high-beta structures. The fifth and sixth columns list the minimum 1 min average field strength B and maximum 1 min average density n within the structures. While the median n of 18 cm^{-3} is less than a factor of two higher than the average value for slow wind, the median B of 0.4 nT is more than a factor of 10 lower. Consistent with the patterns in Figure 2 showing closer control of the beta profiles by B rather than n, what most often makes the high-beta structures extreme events is not high density but rather the excursions of B toward zero since the beta ratio contains the square of B in its denominator.

[26] The seventh column of Table 2 lists whether an elevated n or ion temperature T or both compensate for the decrease in B to achieve (approximate) pressure balance, and the eighth column lists whether the high-beta structure is immersed in a region of relatively high, medium, or low entropy (specific entropy argument $T/n^{2/3}$), where high and low entropy indicate origins in what was originally fast and slow wind, respectively [e.g., *Burlaga et al.*, 1990a; *Burton et al.*, 1999]. Of the 37 structures, 30 have low entropy, implying immersion in slow wind, and these 30 include all 17 cases where primarily n balances B, as might be expected for material stemming from the coronal streamer belt [e.g., *Gosling et al.*, 1981]. Perhaps surprisingly, T rather than n balances B in five of the low-entropy cases, and both balance B in the remaining seven cases. These are the patterns that also characterize the seven cases with high or medium entropy, implying immersion in fast or indeterminate wind: T balances B in three cases, and both T and n balance B in four cases.

3. Discussion

[27] In the steady state view promoted by *Winterhalter et al.* [1994], three features constitute a heliospheric plasma sheet: a sector boundary, a high-beta structure, and a current sheet. To test this concept systematically, one can search for occurrences of one of these features and then test for the other two. Section 2 presents the results of searches for the first two, sector boundaries and high-beta structures. A test based upon a search for the third, current sheets, has essentially already been performed in two parts. First, using Wind data from 1 January to 24 March 1995, A. D. Coleman (unpublished manuscript, 1998) found that 74% of 138 current sheets identified by local polarity reversals in ϕ_B were immersed in high-beta structures. Second, *Szabo et al.* [1999], using Wind data from 1 January to 25 July 1995 and from 3 November 1997 to 17 April 1998, found that most local polarity reversals in ϕ_B did not coincide with sector boundaries identified in electron data. From these two studies we can conclude that most current sheets coincide with high-beta structures but not with sector boundaries. Combined with the findings reported in Section 2, that only half of sector boundaries coincide with current sheets immersed in high-beta structures and that most high-beta structures coincide with current sheets but not with sector

boundaries, it is clear that the heliospheric plasma sheet as a high-beta feature is highly variable. The steady state view applies regularly only in the statistical sense and at the larger scales proposed by *Gosling et al.* [1981] and *Burlaga et al.* [1990a].

[28] There are three aspects to high-beta HPS variability: form, occurrence at some sector boundaries and not at others, and occurrence of identical structures away from sector boundaries. The variability in form is apparent in a comparison between Figures 2a and 2b, where the beta profiles, amplitudes, and scales as well as the variation in ϕ_B across the sector boundary are different. A frequent factor in the variability in occurrence is noncoincidence of sector boundaries and current sheets, as illustrated in Figure 2c. Figure 1 indicates that 17 (33%) of the 52 identified sector boundaries are not classified as having HPSs because they lack current sheets. In many of these cases, unlike those in Figure 2c, the sector boundary is imbedded in a region of gradual transition, in which ϕ_B hovers for many hours near the boundary between toward and away sector directions before making a definite turn into the opposite sector. Noncoincidence of sector boundaries and current sheets is of interest in its own right and forms the subject of another study (Paper 2), as mentioned in section 1. Here, relevant to the interpretation offered below, we note that the intervals of mismatch between true polarity and local field polarity mark field inversions, where field lines turn back on themselves, if not by 180°, at least by more than 90°. Field inversions also must be responsible for the brief local polarity reversals found in high-beta structures that lack true sector boundaries, which embody the third aspect of HPS variability. Since these high-beta structures are the same as HPSs, except for lack of sector boundaries, we include them here in the more general category of "plasma sheets."

[29] *Zurbuchen et al.* [2001] analyzed 12 plasma sheets without sector boundaries, calling them "microscale magnetic holes" (as opposed to kinetic-scale holes, which most likely have a different source mechanism) and found the same properties as reported here. In addition, they found that the composition and charge-state ratios of the densities of Fe/O and O^{7+}/O^{6+} were the same inside the holes, or plasma sheets, as in the ambient wind, implying that they must form high in the corona, above the critical height where the ratios become fixed. *Zurbuchen et al.* [2001] propose that the formation mechanism is interchange reconnection high in the corona between a large coronal loop and an open field line, a process predicted to be ubiquitous as a means of open-field line transport in the model of *Fisk et al.* [1999].

[30] Here we propose a synthesis of the *Zurbuchen et al.* [2001] mechanism and the *Wang et al.* [1998] mechanism of plasma release at the cusps of helmet streamers, described in section 1, as an explanation for all high-beta plasma sheets, with or without sector boundaries. Both mechanisms draw on interchange reconnection high in the corona to release high-density plasma from closed loops. We add that interchange reconnection offers an explanation for the pervasive magnetic field inversions within plasma sheets. Figure 5 is an adaptation of the schematic drawings of *Wang et al.* [1998, 2000] and *Zurbuchen et al.* [2001], illustrating how inversions can occur. In the top panel a dashed open field line approaches a closed helmet streamer field line from behind. The field lines meet at the "X," where they are nearly antiparallel, and reconnect. The second panel shows the configuration following this interchange reconnection. The original loop has interchanged with a smaller loop, the open field line has been transported poleward, and the plasma parcel at the cusp of the original loop now resides on the open field line. More important, the released plasma parcel resides in a kink on the open field line. The field turns back on itself between two localized current sheets marked by dotted lines, and the entire structure convects outward as a transient plasma sheet. The topological configuration is basically the same as that proposed by *Crooker et al.* [2002] for opening closed loops in interplanetary coronal mass ejections, except that the difference in scale between the interchanging loops is much smaller. Since the sector boundary stems from the cusp of the helmet streamer belt (not illustrated), there is enough flexibility in the configuration in Figure 5 to account for the plasma sheets and field inversions observed both at and displaced from sector boundaries.

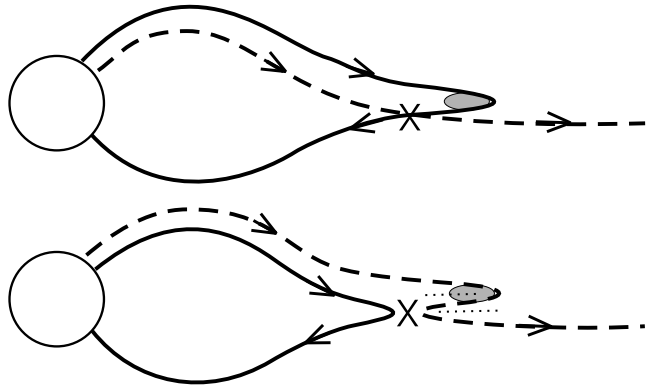

Figure 5. Schematic of high-beta plasma sheet release (shaded parcel) by interchange reconnection near the cusp of a helmet streamer and the resulting field inversion with localized current sheets (dotted lines) (adapted from *Wang et al.* [2000] and *Zurbuchen et al.* [2001]).

[31] An additional point favoring the Figure 5 interpretation is its consistency with the relatively weak density enhancements documented by *Wang et al.* [1998, 2000], usually only 10% above background streamer belt densities, although occasionally rising to 20–30%. As discussed in section 2, the increase in density balancing the drop in field strength to maintain pressure balance is generally a small percent of the total density because the total is usually already elevated on a larger scale.

4. Conclusions

[32] At scales from minutes to a few hours, where elevated beta is its distinguishing characteristic, the heliospheric plasma sheet is highly variable. Its form ranges from minutes-long spikes in beta encompassing the thinnest of current sheets [cf. *Winterhalter et al.*, 1994] to larger beta structures of various amplitudes encompassing complicated current structures. Moreover, half of sector boundaries lack high-beta HPSs, and plasma sheets like the HPS often occur

away from sector boundaries. All of these high-beta plasma sheets may result from the sporadic release of plasma from closed loops in the helmet streamer belt through interchange reconnection with open field lines [*Wang et al.*, 1998, 2000; *Zurbuchen et al.*, 2001]. Interchange reconnection can create the field inversions commonly associated with plasma sheets and their variability.

[33] **Acknowledgments.** This research was supported by the National Science Foundation under grant ATM-0119700 and by NASA under grant NAG5-10856.

[34] Shadia Rifai Habbal thanks Daniel Winterhalter and Yi-Ming Wang for their assistance in evaluating this paper.

References

Bavassano, B., R. Woo, and R. Bruno (1997), Heliospheric plasma sheet and coronal streamers, *Geophys. Res. Lett.*, *24*, 1655–1658.

Borrini, G., J. T. Gosling, S. J. Bame, W. C. Feldman, and J. M. Wilcox (1981), Solar wind helium and hydrogen structure near the heliospheric current sheet: A signal of coronal streamers at 1 AU, *J. Geophys. Res.*, *86*, 4565–4573.

Burlaga, L. F., W. H. Mish, and Y. C. Whang (1990a), Coalescence of recurrent streams of different sizes and amplitudes, *J. Geophys. Res.*, *95*, 4247–4255.

Burlaga, L. F., J. D. Scudder, L. W. Klein, and P. A. Isenberg (1990b), Pressure-balanced structures between 1 AU and 24 AU and their implications for solar wind electrons and interstellar pickup ions, *J. Geophys. Res.*, *95*, 2229–2239.

Burton, M. E., M. Neugebauer, N. U. Crooker, R. von Steiger, and E. J. Smith (1999), Identification of trailing edge solar wind stream interfaces: A comparison of Ulysses plasma and composition measurements, *J. Geophys. Res.*, *104*, 9925–9932.

Crooker, N. U. (2003), Heliospheric current and plasma sheet structure, in *Solar Wind Ten*, edited by M. Velli, R. Bruno, and F. Malara, *AIP Conf. Proc.*, *679*, 93–97.

Crooker, N. U., G. L. Siscoe, S. Shodhan, D. F. Webb, J. T. Gosling, and E. J. Smith (1993), Multiple heliospheric current sheets and coronal streamer belt dynamics, *J. Geophys. Res.*, *98*, 9371–9381.

Crooker, N. U., M. E. Burton, J. L. Phillips, E. J. Smith, and A. Balogh (1996a), Heliospheric plasma sheets as small-scale transients, *J. Geophys. Res.*, *101*, 2467–2474.

Crooker, N. U., M. E. Burton, G. L. Siscoe, S. W. Kahler, J. T. Gosling, and E. J. Smith (1996b), Solar wind streamer belt structure, *J. Geophys. Res.*, *101*, 24,331–24,341. (Correction, *J. Geophys. Res., 102*, 4741, 1997.)

Crooker, N. U., A. J. Lazarus, R. P. Lepping, K. W. Ogilvie, J. T. Steinberg, A. Szabo, and T. G. Onsager (1996c), A two-stream, four-sector, recurrence pattern: Implications from WIND for the 22-year geomagnetic activity cycle, *Geophys. Res. Lett.*, *23*, 1275–1278.

Crooker, N. U., J. T. Gosling, and S. W. Kahler (2002), Reducing heliospheric magnetic flux from coronal mass ejections without disconnection, *J. Geophys. Res.*, *107*(A2), 1028, doi:10.1029/2001JA000236.

Crooker, N. U., D. E. Larson, S. W. Kahler, S. M. Lamassa, and H. E. Spence (2003), Suprathermal electron isotropy in high-beta solar wind and its role in heat flux dropouts, *Geophys. Res. Lett.*, *30*(12), 1619, doi:10.1029/2003GL017036.

Crooker, N. U., S. W. Kahler, D. E. Larson, and R. P. Lin (2004), Large-scale magnetic field inversions at sector boundaries, *J. Geophys. Res.*, *109*, A03108, doi:10.1029/2003JA010278.

Fisk, L. A., T. H. Zurbuchen, and N. A. Schwadron (1999), On the coronal magnetic field: Consequences of large-scale motion, *Astrophys. J.*, *521*, 868–877.

Geiss, J., G. Gloeckler, and R. von Steiger (1995), Origin of the solar wind from composition measurements, *Space Sci. Rev.*, *72*, 49–60.

Gosling, J. T., G. Borrini, J. R. Asbridge, S. J. Bame, W. C. Feldman, and R. T. Hansen (1981), Coronal streamers in the solar wind at 1 AU, *J. Geophys. Res.*, *86*, 5438–5448.

Kahler, S., and R. P. Lin (1994), The determination of interplanetary magnetic field polarities around sector boundaries using $E > 2$ keV electrons, *Geophys. Res. Lett.*, *21*, 1575–1578.

Kahler, S., and R. P. Lin (1995), An examination of directional discontinuities and magnetic polarity changes around interplanetary sector boundaries using $E > 2$ keV electrons, *Sol. Phys.*, *161*, 183–195.

Kahler, S. W., N. U. Crooker, and J. T. Gosling (1996), The topology of intrasector reversals of the interplanetary magnetic field, *J. Geophys. Res.*, *101*, 24,373–24,382.

Lacombe, C., C. Salem, A. Mangeney, J.-L. Steinberg, M. Maksimovic, and J. M. Bosqued (2000), Latitudinal distribution of the solar wind properties in the low- and high-pressure regimes: Wind observations, *Ann. Geophys.*, *18*, 852–865.

Lepping, R. L., et al. (1995), The Wind magnetic field investigation, *Space Sci. Rev.*, *71*, 207–229.

Lin, R. P., et al. (1995), A three-dimensional plasma and energetic particle investigation for the Wind spacecraft, *Space Sci. Rev.*, *71*, 125–153.

Mullan, D. J., C. W. Smith, N. F. Ness, and R. M. Skoug (2003), Short-period magnetic fluctuations in *Advanced Composition Explorer* solar wind data: Evidence for anticorrelation with Alfven speed, *Astrophys. J.*, *583*, 496–505.

Ogilvie, K. W., et al. (1995), SWE: A comprehensive plasma instrument for the Wind spacecraft, *Space Sci. Rev.*, *71*, 55–77.

Schwenn, R. (1990), Large-scale structure of the interplanetary medium, in *Physics of the Inner Heliosphere I*, edited by R. Schwenn and E. Marsch, pp. 99–181, Springer-Verlag, New York.

Szabo, A., D. E. Larson, and R. P. Lepping (1999), The heliospheric current sheet on small scale, in *Solar Wind Nine*, edited by S. Habbal et al., *AIP Conf. Proc.*, *471*, 589–592.

Wang, Y.-M., N. R. Sheeley Jr., J. H. Walters, G. E. Brueckner, R. A. Howard, D. J. Michels, P. L. Lamy, R. Schwenn, and G. M. Simnett (1998), Origin of streamer material in the outer corona, *Astrophys. J.*, *498*, L165–L168.

Wang, Y.-M., N. R. Sheeley Jr., D. G. Socker, R. A. Howard, and N. B. Rich (2000), The dynamical nature of coronal streamers, *J. Geophys. Res.*, *105*, 25,133–25,142.

Winterhalter, D., E. J. Smith, M. E. Burton, N. Murphy, and D. J. McComas (1994), The heliospheric plasma sheet, *J. Geophys. Res.*, *99*, 6667–6680.

Zurbuchen, T. H., S. Hefti, L. A. Fisk, G. Gloeckler, N. A. Schwadron, C. W. Smith, N. F. Ness, R. M. Skoug, D. J. McComas, and L. F. Burlaga (2001), On the origin of microscale magnetic holes in the solar wind, *J. Geophys. Res.*, *106*, 16,001–16,010.

N. U. Crooker, C.-L. Huang, S. M. Lamassa, and H. E. Spence, Center for Space Physics, Boston University, 725 Commonwealth Avenue, Boston, MA 02215, USA. (crooker@bu.edu; hcl@bu-ast.bu.edu; slamassa@yahoo.com; spence@bu.edu)

S. W. Kahler, Air Force Research Laboratory, 29 Randolph Road, Hanscom AFB, MA 01731-3010, USA. (stephen.kahler@hanscom.af.mil)

D. E. Larson, Space Sciences Laboratory, University of California, Berkeley, Berkeley, CA 94720-7450, USA. (davin@ssl.berkeley.edu)